Macromolecules

pubs.acs.org/Macromolecules Article

CO_2-Involved and Isocyanide-Based Three-Component Polymerization toward Functional Heterocyclic Polymers with Self-Assembly and Sensing Properties

Dongming Liu, Bo Song, Jia Wang, Baoxi Li, Bingnan Wang, Mingzhao Li, Anjun Qin,* and Ben Zhong Tang*

Cite This: *Macromolecules* 2021, 54, 4112–4119 Read Online

ACCESS | Metrics & More | Article Recommendations | Supporting Information

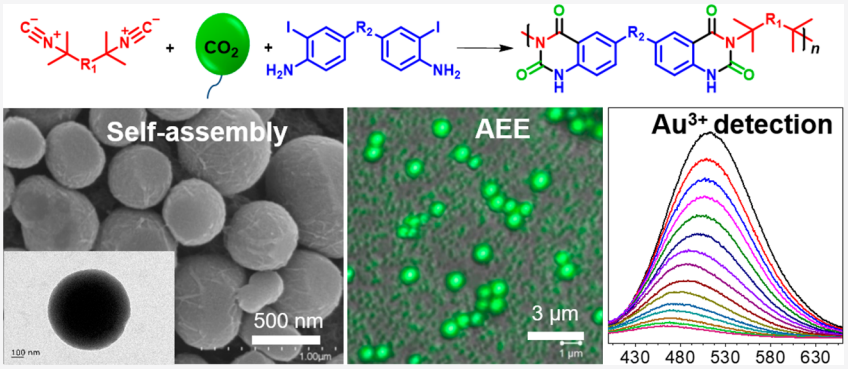

ABSTRACT: CO_2 utilization has been a hot research topic in academic and industrial fields. Besides converting CO_2 into chemicals and fuels, incorporating it into the polymers to construct functional materials is another promising strategy. However, the CO_2-involved polymerization techniques should be further developed. In this work, a facile and efficient CO_2-involved multicomponent polymerization is successfully developed. The reaction of monomers of CO_2, isocyanides, and 2-iodoanilines readily produces soluble and thermally stable poly(benzoyleneurea)s with well-defined structures under mild conditions. Thanks to the formed amide groups in the heterocyclic units of the main chains, the resultant polymers could self-assemble into spheres with sizes between 200 and 1000 nm. The polymers containing tetraphenylethylene (TPE) units show the unique aggregation-enhanced emission (AEE) features, which could be used to visualize the self-assembly process and morphologies under UV irradiation, and serve as fluorescent probes to selectively and sensitively detect Au^{3+} ions. Notably, the polymers containing *cis*- and *trans*-TPE units exhibit different behaviors in self-assembly and limits of detection for Au^{3+} ions due to the different intermolecular interactions. Thus, this work not only provides a new strategy for CO_2 utilization but also furnishes a series of functional heterocyclic polymers for diverse applications.

INTRODUCTION

In the past few decades, the conversion and utilization of abundant, non-toxic, and renewable carbon dioxide (CO_2) have become a hot topic in both academic and industrial fields.[1−6] Although CO_2 possesses thermodynamic stability and kinetic inertness, a large number of works on converting CO_2 into chemicals and fuels via the constructions of C−O, C−N, C−C, and C−H bonds have been reported.[7−10] Meanwhile, the transformation of CO_2 into functional polymers is receiving considerable attention in polymer chemistry. However, most of the reports are mainly focused on the preparation of chain polymers.[11−20] It is very challenging to synthesize heterocyclic polymers by CO_2-involved polymerization.

Generally, the preparation of heterocyclic polymers from CO_2-involved polymerizations can be achieved via the following two strategies: (1) first transforming CO_2 into other monomers, such as 3-ethylidene-6-vinyltetrahydro-2*H*-pyran-2-one (EVL)[21−23] and five-membered cyclic carbonates (5CC)s;[24,25] (2) directly using CO_2 as a monomer. The latter is preferred, and elegant works have been done. For example, Tsuda and co-workers reported a nickel complex-catalyzed alternating copolymerization of CO_2 and diynes toward poly(2-pyrones).[26,27] However, the copolymerization was

Received: February 9, 2021
Revised: March 27, 2021
Published: April 19, 2021

https://doi.org/10.1021/acs.macromol.1c00312
Macromolecules 2021, 54, 4112–4119

carried out under high pressure (20−50 bar). In 2012, Li and co-workers developed a multicomponent polycoupling of benzaldehyde, 1,4-diethynylbenzene, 1,6-hexadiamine, and CO_2.[28] However, the resultant polyoxazolidinones showed poor solubility, which hinders their further property study and application exploration. In 2018, Dong and co-workers reported a catalyst-free multicomponent spiropolymerization of diisocyanides, alkynes, and CO_2 and soluble spiropolymers were successfully obtained.[29] Our group has also developed a three-component polymerization of CO_2, bis(propargylic alcohol)s, and aryl dihalides under atmospheric pressure recently.[30] Nevertheless, these polymerizations could only obtain oxygen-containing heterocyclic polymers. Therefore, we anticipate that distinctive monomers such as isocyanides can be incorporated in CO_2-involved polymerizations under mild reaction conditions toward novel heterocyclic polymers.

Isocyanides have been widely used to construct heterocycles.[31,32] Thanks to the widespread applications of isocyanides in multicomponent reactions (MCRs)[33−35] and according to the reported works,[36−38] we hypothesize that a novel multicomponent polymerization (MCP) based on the monomers of CO_2 and isocyanides could be established under mild reaction conditions, from which heterocyclic polymers could be readily generated and unique properties could be found. Indeed, after a systematical investigation, an MCP of CO_2, diisocyanides, and bis(2-iodoaniline)s was developed and a series of poly(benzoyleneurea)s with well-defined structures were constructed. Thanks to the containing amide groups, the resultant polymers could self-assemble into solid spheres and the polymers bearing tetraphenylethylene (TPE) moieties showed the unique aggregation-enhanced emission (AEE) characteristic, which could be used as a fluorescent probe to sensitively detect Au^{3+} ions.

RESULTS AND DISCUSSION

Monomer Synthesis. Diisocyanides **1a** and **1b** (Schemes S1 and S2) were prepared according to the synthetic procedures in the literature.[39−41] Inspired by the preparation method of 2-iodoaniline,[42,43] bis(2-iodoaniline)s **2a−2d** (Schemes S3 and S4) were prepared for the first time as far as we know.

Model Reaction. Before exploration of the CO_2-involved and isocyanide-based polymerization, the model reaction was carried out using CO_2, 2-iodoanilines, and *tert*-butyl isocyanide as the reactants following the reported procedures (Scheme S5).[37] The three-component reaction proceeded smoothly in the presence of the catalytic system of palladium chloride ($PdCl_2$), triphenylphosphine (PPh_3), and 1,8-diazabicyclo[5.4.0]undec-7-ene (DBU) in *N*,*N*-dimethylacetamide (DMAc) under atmospheric pressure CO_2, which generated model compound **3** in 90% yield. The structure of **3** was characterized by Fourier transform infrared (FT-IR) (Figure 1C) and ^{1}H and ^{13}C NMR (Figures 2C and 3C) spectroscopies, and satisfactory results were obtained.

Polymerization. Encouraged by the positive results of the above highly efficient model reaction, we set out to develop relevant MCP (Scheme 1). Herein, **1a** and **2a** were chosen as representative monomers to systematically investigate the polymerization conditions.

First, we investigated the effect of solvents on the polymerizations. Among the used solvents of tetrahydrofuran (THF), toluene, acetonitrile, 1,2-dichloroethane (DCE), dimethyl sulfoxide (DMSO), *N*,*N*-dimethylformamide (DMF), and DMAc, a superior polymerization result was obtained in DMAc, furnishing a soluble polymer with a weight-average molecular weight (M_w) of 6500 in 82% yield (Table S1). The results suggest that high polarity solvents could favor this polymerization because they can well dissolve the resultant products.

Second, we studied the effect of catalysts and the DBU loading on the polymerization. Among the testing catalysts, $PdCl_2$/PPh_3 was the most efficient one (Table S2), and the

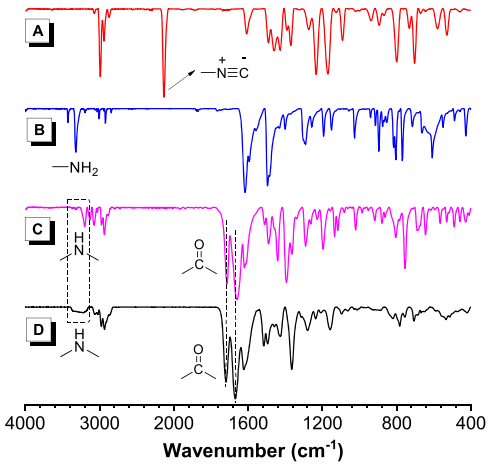

Figure 1. FT-IR spectra of (A) isocyanide **1a**, (B) 2-iodoaniline **2b**, (C) model compound **3**, and (D) P**1a**/**2b**/CO_2.

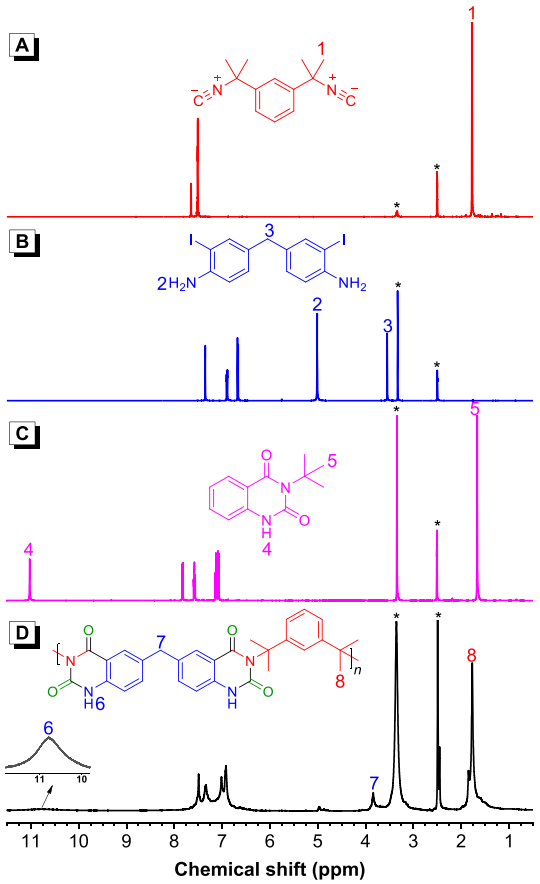

Figure 2. ^{1}H NMR spectra of (A) monomer **1a**, (B) monomer **2b**, (C) model compound **3**, and (D) P**1a**/**2b**/CO_2 in DMSO-d_6. The solvent peaks are marked with asterisks.

https://doi.org/10.1021/acs.macromol.1c00312
Macromolecules 2021, 54, 4112−4119

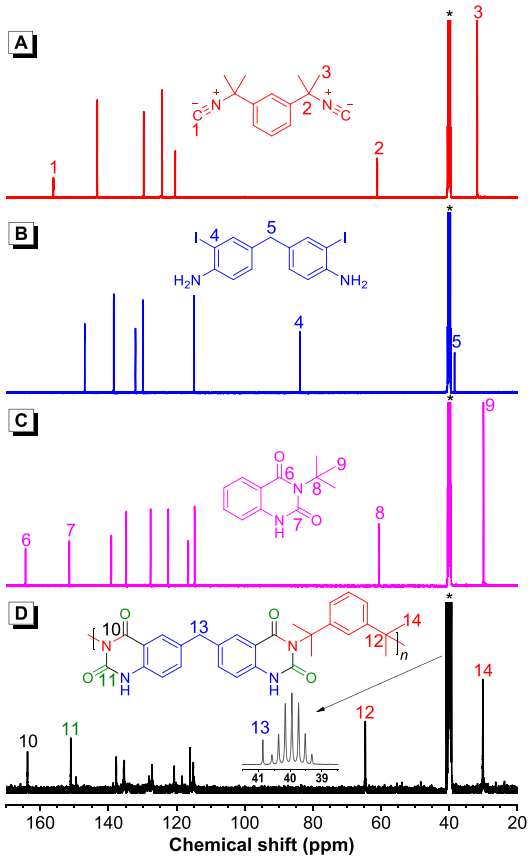

Figure 3. ^{13}C NMR spectra of (A) monomer **1a**, (B) monomer **2b**, (C) model compound **3**, and (D) P**1a**/**2b**/CO_2 in DMSO-d_6. The solvent peaks are marked with asterisks.

Scheme 1. Multicomponent Polymerization of CO_2, Diisocyanides, and Bis(2-iodoaniline)s in the Presence of $PdCl_2$, PPh_3, and DBU under Atmospheric Pressure

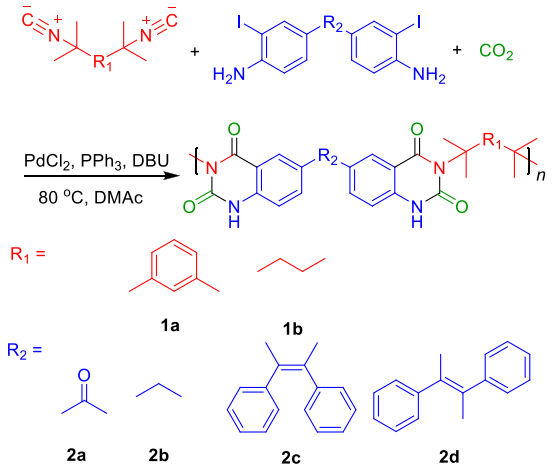

highest catalytic activity for this polymerization was obtained in the presence of 15 mol % $PdCl_2$ and 30 mol % PPh_3 (Table S3). Notably, the DBU loading plays a significant role in the polymerization. A poor result was obtained when the amount of DBU decreased from 3 to 2 equiv. of monomers (Table S4, entry 1). Hence, 15 mol % $PdCl_2$, 30 mol % PPh_3, and 3 equiv. of DBU were chosen for the following polymerizations.

Third, the effect of temperature on the polymerization was explored. As depicted in Table S5, the results showed that the polymer with a higher M_w was obtained in 83% yield at 80 °C (Table S5, entry 2). By increasing the polymerization temperature to 90 °C, no obvious increment in the M_w and yield was observed. We thus used 80 °C as the optimal polymerization temperature.

Fourth, we tested the effect of monomer concentration on the polymerization, and the results are shown in Table S6. It was found that the M_w values and yields of resultant polymers enhanced first and then decreased when the concentration of **1a** increased from 0.05 to 0.4 M. Taking the yield and M_w into consideration, we chose 0.1 M as the monomer concentration.

Fifth, we screened the time course on the polymerization (Table S7). The yields and M_w values of the resultant polymers gradually increased with the extension of polymerization time and reached the maximum of 86% and 8700 at 18 h, respectively. Further prolonging the reaction time to 24 h led to a slight decrease in the yield of the product. Therefore, we used 18 h as the reaction time.

Finally, we investigated the effect of CO_2 pressure on the polymerization. As shown in Table S8, increasing the pressure from 1 to 4 and 10 atm, the M_w values of the resultant polymers slightly increased, but the yields decreased sharply. Thus, we chose 1 atm (balloon) as the experimental pressure, which greatly facilitates further application of this polymerization.

With these optimal polymerization conditions in hand, we polymerized different diisocyanides **1** and bis(2-iodoaniline)s **2** monomers under atmospheric pressure CO_2 to verify their robustness and universality. The results showed that all the polymerizations proceeded smoothly, furnishing corresponding polymers with acceptable M_w values (up to 8700) in satisfactory yields (up to 86%) (Table 1 and Figure S1). The relatively low molecular weights of the polymers might be due to the low reactivity of the used isocyanide monomers

Table 1. Polymerization Results of Diisocyanides 1, Bis(2-iodoaniline)s 2, and CO_2[a]

entry	monomer	polymer	yield (%)	M_w[b]	M_n[b]	n	$Đ$[b]
1	**1a** + **2a** + CO_2	P**1a**/**2a**/CO_2	86	8700	4800	10	1.81
2	**1a** + **2b** + CO_2	P**1a**/**2b**/CO_2	80	7500	4400	9	1.70
3	**1a** + **2c** + CO_2	P**1a**/**2c**/CO_2	73	6700	4300	7	1.56
4	**1a** + **2d** + CO_2	P**1a**/**2d**/CO_2	84	7100	4200	7	1.69
5	**1b** + **2a** + CO_2	P**1b**/**2a**/CO_2	64	7700	4700	11	1.64
6	**1b** + **2b** + CO_2	P**1b**/**2b**/CO_2	69	5600	4000	9	1.40
7	**1b** + **2c** + CO_2	P**1b**/**2c**/CO_2	54	6000	4200	7	1.43
8	**1b** + **2d** + CO_2	P**1b**/**2d**/CO_2	60	6300	4300	7	1.47

[a]Carried out in DMAc at 80 °C under atmosphere CO_2 (balloon) for 18 h in the presence of $PdCl_2$, PPh_3, and DBU. [**1**] = 0.10 M. [**1**]/[**2**]/[$PbCl_2$]/[PPh_3]/[DBU] = 1:1:0.15:0.3:3. [b]Estimated by GPC with DMF containing 0.05 M LiBr as an eluent on the basis of linear polymethyl methacrylate (PMMA) calibration; $Đ$, polydispersity index (M_w/M_n, M_w, weight-average molecular weight; M_n, number-average molecular weight; n, the number of repeating units).

https://doi.org/10.1021/acs.macromol.1c00312
Macromolecules 2021, 54, 4112−4119

connected with the bulky groups. Notably, besides the precipitation, the catalyst residues could be further removed following the method given in the literature.[44]

Due to the strong hydrogen bonding interactions among the formed amide groups, the resultant polymers showed poor solubility in less polar solvents, such as THF and DCE, but could be fully dissolved in highly polar organic solvents of DMAc, DMF, DMSO, 1,1,1,3,3,3-hexafluoro-2-propanol (HFIP), *etc*. They also exhibited good thermal stability. The thermogravimetric analysis (TGA) measurement revealed that the temperatures for 5% weight loss (T_d) of the polymers are in the range of 205−246 °C (Figure S2).

Structural Characterization. To obtain the structural information of resultant polymers, FT-IR and NMR spectroscopy measurements were carried out. Since P**1a**/**2b**/CO_2 could provide more characteristic structural information, we thus selected it as a representative example for the discussion of the structural characterization.

In the FT-IR spectra (Figure 1), the strong stretching vibration of $-N^+{\equiv}C^-$ in **1a** appeared at 2143 cm^{-1} and that of $-NH_2$ in **2b** was observed at 3436 and 3326 cm^{-1}. However, in the spectra of model compound **3** and P**1a**/**2b**/CO_2, these peaks were hardly observed, indicating that the monomers were consumed. Meanwhile, new peaks of −NH in the spectra of **3** and P**1a**/**2b**/CO_2 emerged at 3204 and 3275 cm^{-1}, respectively, and new peaks assigned to the two C═O peaks in the structure of benzoyleneurea appeared at 1715 and 1671 cm^{-1}. These results suggest that the MCP of CO_2, isocyanides, and 2-iodoanilines proceeded well.

More detailed information of the polymer structures can be acquired from the NMR spectra. As shown in Figure 2, in the ^{1}H NMR spectra, the resonances of methyl proton in **1a** and the methylene one in **2b** remained in the model compound **3** and P**1a**/**2b**/CO_2. However, primary amine protons of **2b** at δ 5.01 were almost absent in the spectra of **3** and P**1a**/**2b**/CO_2, indicating that **2b** was almost completely consumed. Meanwhile, new peaks at δ 11.01 and 10.8 in the spectra of **3** and P**1a**/**2b**/CO_2 could be ascribed to the resonance of the amidic protons of benzoyleneurea units.

The ^{13}C NMR analysis further confirmed the polymer structures. As shown in Figure 3, the characteristic carbons of isocyanide groups in **1a** and those adjacent to the iodine groups in **2b** resonated at δ 156.25 and 84.02, respectively. However, they disappeared in the spectra of **3** and P**1a**/**2b**/CO_2, demonstrating that the monomers were consumed. At the same time, two new peaks at δ 163.6 and 151.1 appeared, which are readily assignable to the resonances of the two newly formed carbonyl carbons of poly(benzoyleneurea)s. Notably, other peaks in the monomers could be found at almost the same positions in the polymers. The spectral profiles of other polymers are similar, which are provided in Figures S3−S23. These spectral characterizations confirm that the MCP of CO_2, isocyanides, and 2-iodoanilines was successfully established and poly(benzoyleneurea)s with defined structures were generated.

Self-Assembly Property. Structurally, our resultant poly(benzoyleneurea)s contain two amide groups in one repeating unit, in which the N—H···O═C hydrogen bonding interactions will facilitate the construction of molecular assemblies.[45,46] In this regard, the self-assembly properties of poly(benzoyleneurea)s were studied. The results showed that all the polymers could form spherical structures with the volatilization of the solvent of DMF (Figure 4 and Figure S24).

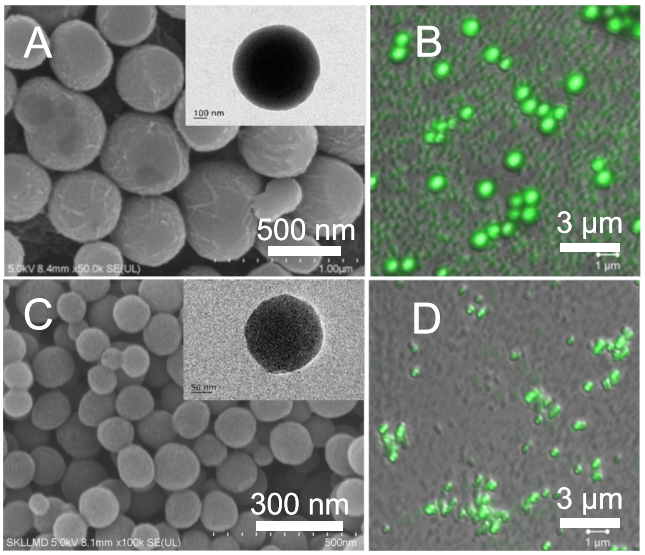

Figure 4. Scanning electron microscopy (SEM) and CLSM images of (A, B) P**1a**/**2c**/CO_2 and (C, D) P**1a**/**2d**/CO_2.The spheres were fabricated by the evaporation of their DMF solutions (concentration: 0.5 mg/mL). Excitation wavelength for the CLSM images: 405 nm. Inset in panels (A, C): TEM images.

Furthermore, their size distribution ranges between 200 and 1000 nm. To furnish the self-assembled micro/nanostructure spheres with functionalities, we incorporated a TPE moiety, a typical unit featuring the aggregation-induced emission (AIE) characteristics, into the polymers to enable them with fluorescence.[47,48] Thanks to their high polarity, **2c** and **2d** containing *cis*- and *trans*-TPE could be isolated, from which P**1a**/**2c**/CO_2 and P**1a**/**2d**/CO_2 were prepared (Scheme 1), and the self-assembly during solvent volatilization could be clearly visualized by confocal laser scanning microscopy (CLSM) (Figure S25). Owing to the containing TPE units, the P**1a**/**2c**/CO_2 and P**1a**/**2d**/CO_2 showed the unique AEE features (Figure 5 and Figure S26). For example, P**1a**/**2c**/CO_2 emitted weakly at 496 nm in DMF solution. With the addition of a poor solvent of water, the emission enhanced gradually due to the restriction of intramolecular motion of the TPE units and the maximum photoluminescence (PL) intensity was recorded in a DMF/water mixture with an 80% water fraction, which was 3.7-fold higher than that in DMF.

Interestingly, the size of the spheres of the P**1a**/**2c**/CO_2 was bigger than that of the P**1a**/**2d**/CO_2 (Figure 4). To have a deep insight into the different self-assembly behaviors, the model compounds **4** and **5** were prepared in yields of 75 and 83%, respectively (Scheme S6). The single crystals of **4** (CCDC 2013880) and **5** (CCDC 2014002) showed that they manifested a highly twisted conformation (Figure 6A,B), and numerous intermolecular hydrogen binding interactions were observed. As seen in Figure 6C, the N—H···O═C interaction (1.917 Å) in the *cis*-isomer **4** was stronger than that (1.970 Å) in *trans*-isomer **5** and the packing of the former was tighter than that of the latter (Figure S27). Thus, the supramolecular interactions of P**1a**/**2c**/CO_2 are stronger than those of P**1a**/**2d**/CO_2, which could be the reason for the smaller self-assembly sizes of P**1a**/**2d**/CO_2.

Next, we investigated the solvent effect on the self-assembly by taking P**1a**/**2d**/CO_2 as a model polymer. The assemblies of the polymer could form large connected void net structures in HFIP, probably because its polarity is too strong to destroy the

https://doi.org/10.1021/acs.macromol.1c00312
Macromolecules 2021, 54, 4112−4119

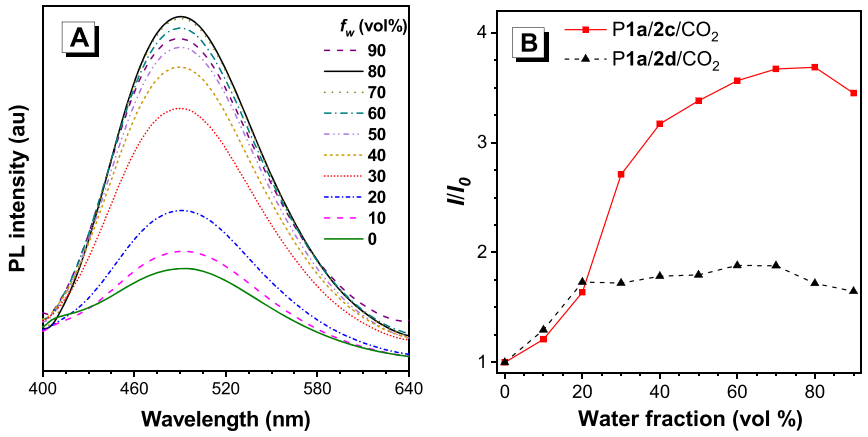

Figure 5. (A) PL spectra of P**1a**/**2c**/CO_2 in DMF/water mixtures with different water fractions. Concentration: 10 μM. λ_{ex}: 340 nm. (B) Plot of the relative PL intensity (I/I_0) of P**1a**/**2c**/CO_2 and P**1a**/**2d**/CO_2 versus the water fraction in DMF/water mixtures, where I is the emission peak intensity in the mixtures and I_0 is the peak intensity in DMF.

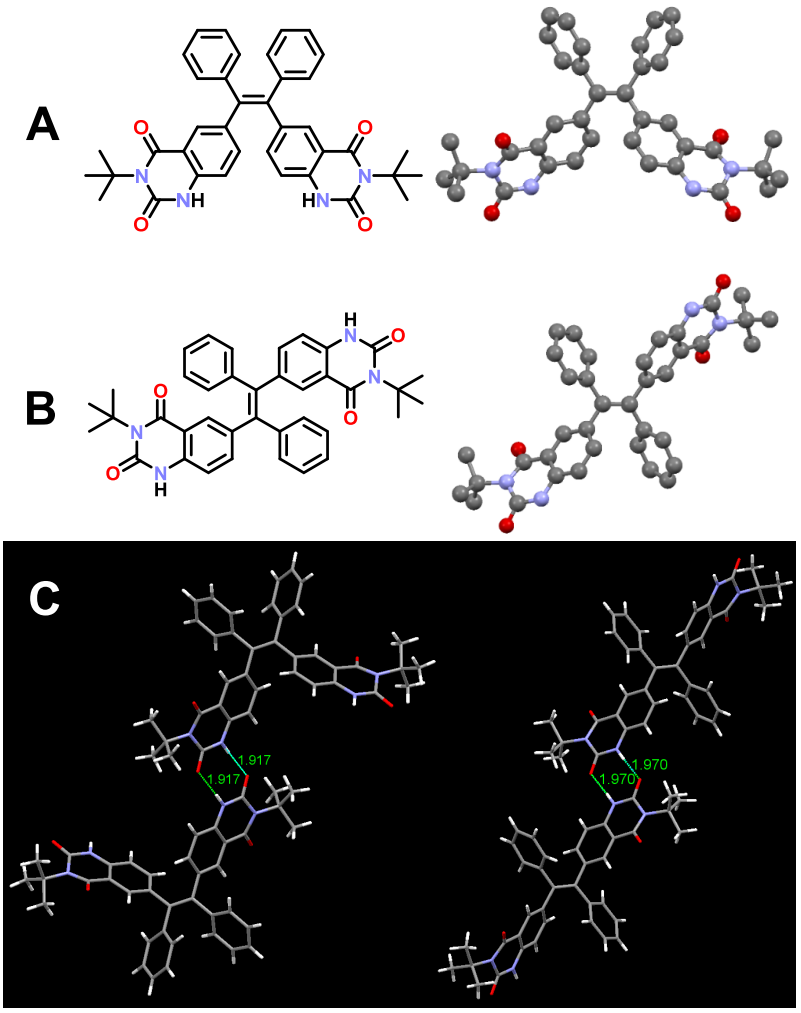

Figure 6. Crystal structures of **4** (A) and **5** (B) and the intermolecular hydrogen bonding interactions in their crystals (C).

intermolecular hydrogen bonding interactions of polymer chains (Figure 7A). Meanwhile, regular and uniform spherical structures were obtained in DMSO, DMF, and DMAc (Figure 7B–E). Interestingly, spheres with a smaller size could be gained via rapid solution precipitation (Figure 7F). These results suggest that the self-assembly could be fine-tuned through solvent and assembly methods.

Gold Ion Detection. Thanks to their AEE features and possible coordination effects, P**1a**/**2c**/CO_2 and P**1a**/**2d**/CO_2 could be applied in the detection of Au^{3+} ions. Despite the interesting chemical and medicinal properties of Au^{3+} ions, their soluble salts could cause cell toxicity in living organisms arising from the strong binding with biomolecules such as DNA and enzymes.[49,50] Based on the wide usage in catalysis

https://doi.org/10.1021/acs.macromol.1c00312
Macromolecules 2021, 54, 4112–4119

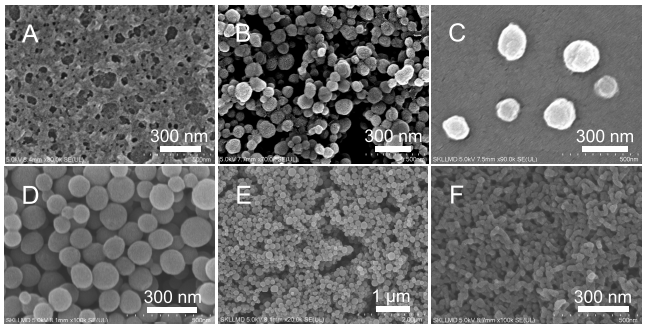

Figure 7. SEM images of P**1a**/**2d**/CO_2 on silicon wafers fabricated by direct vaporization of the solutions of (A) HFIP, (B) DMSO, (C) DMAc, and (D, E) DMF solution (concentration: 0.5 mg/mL) and by (F) fast injection of DMF solution into methanol.

and the toxicity associated with Au^{3+}, it is necessary to develop fluorescent probes with high sensitivity and selectivity for Au^{3+}.[51]

First, we investigated the selectivity of P**1a**/**2c**/CO_2 towards 13 different kinds of metal ions including Au^{3+}, Pt^{4+}, Rh^{3+}, Ru^{3+}, Zn^{2+}, Ni^{2+}, Pb^{2+}, Cd^{2+}, Cu^{2+}, Mn^{2+}, Co^{2+}, Cr^{3+}, and Ag^{+}. As shown in Figure 8, the PL intensity of P**1a**/**2c**/CO_2 in

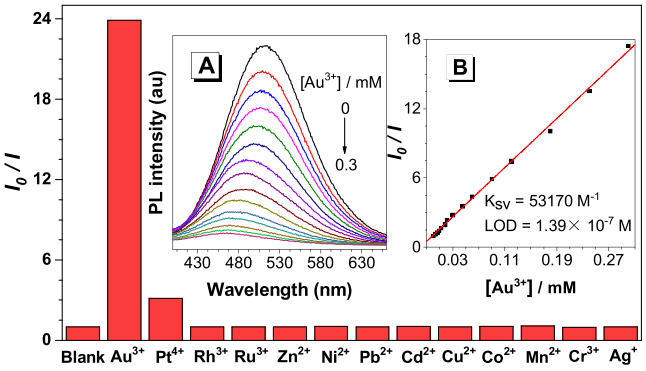

Figure 8. Selective detection of Au^{3+} by P**1a**/**2c**/CO_2 in DMF/water mixtures with an 80% water fraction among 13 kinds of metal ions. [P**1a**/**2c**/CO_2] = 10^{-6} M, [metal ion] = 5×10^{-5} M. Inset: (A) PL spectra of the P**1a**/**2c**/CO_2 in the DMF/water mixture with an f_w of 80% with different Au^{3+} concentrations. λ_{ex}: 340 nm. (B) Stern–Volmer plots of I_0/I of P**1a**/**2c**/CO_2 solution versus Au^{3+} concentration, where I is the peak intensity and I_0 is the peak intensity at [Au^{3+}] = 0.

DMF/water mixtures with a f_w of 80% showed no obvious changes after the addition of other metal ions except for a remarkable reduction upon Au^{3+} ions, demonstrating that P**1a**/**2c**/CO_2 could selectively detect Au^{3+} ions.

Then, we studied a possible sensing mechanism. No new peak occurred in the absorption spectra of the polymer upon gradually adding Au^{3+} ions (Figure S28A). Moreover, the lifetime of the polymer in the presence of the Au^{3+} ions became shorter (Figure S28B). These results suggest that a dynamic quenching might occur. In addition, the PL spectrum of the polymer barely overlapped with the absorption spectrum of Au^{3+} ions (Figure S29). Thus, the PL quenching could be attributed to the coordination interactions of P**1a**/**2c**/CO_2 with the Au^{3+} ions by the formation of supramolecular species.[52]

Another important parameter for a chemosensor is its sensitivity. We then tested the sensitivity of our polymer toward Au^{3+} ions. The PL intensity gradually weakened with the addition of Au^{3+} ions (Figure 8A). When the concentration of Au^{3+} ions was lower than 0.30 mM, the Stern–Volmer plot of P**1a**/**2c**/CO_2 showed a linear relationship, from which a quenching constant of 53,170 M^{-1} was deduced (Figure 8B). The limit of detection (LOD) was calculated to be 1.39×10^{-7} M (ca. 0.027 $\mu g \cdot mL^{-1}$), which is far below the Au^{3+} toxicity values (6–75 $\mu g \cdot L^{-1}$) for various aquatic organisms,[53] indicating its potential application in Au^{3+} detection in an aquatic ecosystem. Notably, P**1a**/**2d**/CO_2 could also be used to detect Au^{3+} ions but with a higher LOD of 9.49×10^{-7} M (Figures S30 and S31), presumably due to the weaker hydrogen-bonding interaction than P**1a**/**2c**/CO_2.

CONCLUSIONS

In this work, we have successfully developed an efficient three-component polymerization of CO_2, isocyanides, and 2-iodoanilines, and soluble and thermally stable poly(benzoyleneurea)s with well-defined structures were constructed under mild reaction conditions for the first time. Thanks to the hydrogen bonding interactions of the formed amide groups, the polymers could self-assemble into spheres with sizes of 200–1000 nm. Moreover, the TPE-containing polymers show the unique AEE features, enabling them to be used to visualize the self-assembly processes and act as fluorescent probes to selectively and sensitively detected Au^{3+} ions. Thus, this work not only offers a new strategy for CO_2 utilization but also provides perspective for the design and synthesis of heterocyclic polymers from CO_2 and isocyanides.

ASSOCIATED CONTENT

Supporting Information

The Supporting Information is available free of charge at https://pubs.acs.org/doi/10.1021/acs.macromol.1c00312.

Materials and instruments; details of synthesis; polymerization condition optimization; and characterization data (TGA, FT-IR, NMR, UV, PL, SEM, CLSM, etc.) (PDF)

X-ray crystal details of **4** (CIF)

X-ray crystal details of **5** (CIF)

AUTHOR INFORMATION

Corresponding Authors

Anjun Qin – *State Key Laboratory of Luminescent Materials and Devices, Guangdong Provincial Key Laboratory of Luminescence from Molecular Aggregates, SCUT-HKUST Joint Research Institute, AIE Institute, Center for Aggregation-Induced Emission, South China University of Technology (SCUT), Guangzhou 510640, China;* orcid.org/0000-0001-7158-1808; Email: msqinaj@scut.edu.cn

Ben Zhong Tang – *State Key Laboratory of Luminescent Materials and Devices, Guangdong Provincial Key Laboratory of Luminescence from Molecular Aggregates, SCUT-HKUST Joint Research Institute, AIE Institute, Center for Aggregation-Induced Emission, South China University of Technology (SCUT), Guangzhou 510640, China; Department of Chemistry, Hong Kong Branch of Chinese National Engineering Research Center for Tissue Restoration and Reconstruction, Institute for Advanced Study, and Department of Chemical and Biological Engineering, The Hong Kong University of Science & Technology (HKUST), Hong Kong 999077, China;* orcid.org/0000-0002-0293-964X; Email: tangbenz@ust.hk

https://doi.org/10.1021/acs.macromol.1c00312
Macromolecules 2021, 54, 4112–4119

Authors

Dongming Liu − *State Key Laboratory of Luminescent Materials and Devices, Guangdong Provincial Key Laboratory of Luminescence from Molecular Aggregates, SCUT-HKUST Joint Research Institute, AIE Institute, Center for Aggregation-Induced Emission, South China University of Technology (SCUT), Guangzhou 510640, China*

Bo Song − *State Key Laboratory of Luminescent Materials and Devices, Guangdong Provincial Key Laboratory of Luminescence from Molecular Aggregates, SCUT-HKUST Joint Research Institute, AIE Institute, Center for Aggregation-Induced Emission, South China University of Technology (SCUT), Guangzhou 510640, China*

Jia Wang − *State Key Laboratory of Luminescent Materials and Devices, Guangdong Provincial Key Laboratory of Luminescence from Molecular Aggregates, SCUT-HKUST Joint Research Institute, AIE Institute, Center for Aggregation-Induced Emission, South China University of Technology (SCUT), Guangzhou 510640, China;* orcid.org/0000-0001-5851-3579

Baoxi Li − *State Key Laboratory of Luminescent Materials and Devices, Guangdong Provincial Key Laboratory of Luminescence from Molecular Aggregates, SCUT-HKUST Joint Research Institute, AIE Institute, Center for Aggregation-Induced Emission, South China University of Technology (SCUT), Guangzhou 510640, China*

Bingnan Wang − *State Key Laboratory of Luminescent Materials and Devices, Guangdong Provincial Key Laboratory of Luminescence from Molecular Aggregates, SCUT-HKUST Joint Research Institute, AIE Institute, Center for Aggregation-Induced Emission, South China University of Technology (SCUT), Guangzhou 510640, China*

Mingzhao Li − *State Key Laboratory of Luminescent Materials and Devices, Guangdong Provincial Key Laboratory of Luminescence from Molecular Aggregates, SCUT-HKUST Joint Research Institute, AIE Institute, Center for Aggregation-Induced Emission, South China University of Technology (SCUT), Guangzhou 510640, China*

Complete contact information is available at: https://pubs.acs.org/10.1021/acs.macromol.1c00312

Notes

The authors declare no competing financial interest.

■ ACKNOWLEDGMENTS

This work was financially supported by the National Natural Science Foundation of China (21788102 and 21525417), the Natural Science Foundation of Guangdong Province (2019B030301003 and 2016A030312002), and the Innovation and Technology Commission of Hong Kong (ITCC-NERC14S01).

■ REFERENCES

(1) Castro, S.; Albo, J.; Irabien, A. Photoelectrochemical Reactors for CO_2 Utilization. *ACS Sustainable Chem. Eng.* **2018**, *6*, 15877−15894.

(2) Bahari, N. A.; Wan Isahak, W. N. R.; Masdar, M. S.; Yaakob, Z. Clean Hydrogen Generation and Storage Strategies via CO_2 Utilization into Chemicals and Fuels: A Review. *Int. J. Energ. Res.* **2019**, *43*, 5128−5150.

(3) Zhang, Z.; Pan, S. Y.; Li, H.; Cai, J.; Olabi, A. G.; Anthony, E. J.; Manovic, V. Recent Advances in Carbon Dioxide Utilization. *Renew. Sust. Energ. Rev.* **2020**, *125*, 109799.

(4) Liu, Q.; Wu, L.; Jackstell, R.; Beller, M. Using Carbon Dioxide as a Building Block in Organic Synthesis. *Nat. Commun.* **2015**, *6*, 5933.

(5) Dabral, S.; Schaub, T. The Use of Carbon Dioxide (CO_2) as a Building Block in Organic Synthesis from an Industrial Perspective. *Adv. Synth. Catal.* **2019**, *361*, 223−246.

(6) Wang, J.; Qin, A.; Tang, B. Z. Multicomponent Polymerizations Involving Green Monomers. *Macromol. Rapid Commun.* **2020**, *53*, 2516−2525.

(7) Huang, K.; Sun, C. L.; Shi, Z. J. Transition-Metal-Catalyzed C-C Bond Formation through the Fixation of Carbon Dioxide. *Chem. Soc. Rev.* **2011**, *40*, 2435−2452.

(8) Cokoja, M.; Bruckmeier, C.; Rieger, B.; Herrmann, W. A.; Kühn, F. E. Transformation of Carbon Dioxide with Homogeneous Transition-Metal Catalysts: A Molecular Solution to a Global Challenge? *Angew. Chem., Int. Ed.* **2011**, *50*, 8510−8537.

(9) Cherubini-Celli, A.; Mateos, J.; Bonchio, M.; Dell'Amico, L.; Companyó, X. Transition Metal-Free CO_2 Fixation into New Carbon-Carbon Bonds. *ChemSusChem* **2018**, *11*, 3056−3070.

(10) Yang, Z. Z.; He, L. N.; Gao, J.; Liu, A. H.; Yu, B. Carbon Dioxide Utilization with C−N Bond Formation: Carbon Dioxide Capture and Subsequent Conversion. *Energy Environ. Sci.* **2012**, *5*, 6602−6639.

(11) Chen, Z.; Hadjichristidis, N.; Feng, X.; Gnanou, Y. Cs_2CO_3-Promoted Polycondensation of CO_2 with Diols and Dihalides for the Synthesis of Miscellaneous Polycarbonates. *Polym. Chem.* **2016**, *7*, 4944−4952.

(12) Chen, Z.; Hadjichristidis, N.; Feng, X.; Gnanou, Y. Poly(urethane−carbonate)s from Carbon Dioxide. *Macromolecules* **2017**, *50*, 2320−2328.

(13) Li, Y.; Zhang, Y. Y.; Hu, L. F.; Zhang, X. H.; Du, B. Y.; Xu, J. T. Carbon Dioxide-Based Copolymers with Various Architectures. *Prog. Polym. Sci.* **2018**, *82*, 120−157.

(14) Song, B.; He, B.; Qin, A.; Tang, B. Z. Direct Polymerization of Carbon Dioxide, Diynes, and Alkyl Dihalides under Mild Reaction Conditions. *Macromolecules* **2017**, *51*, 42−48.

(15) Wu, P. X.; Cheng, H. Y.; Shi, R. H.; Jiang, S.; Wu, Q. F.; Zhang, C.; Arai, M.; Zhao, F. Y. Synthesis of Polyurea via the Addition of Carbon Dioxide to a Diamine Catalyzed by Organic and Inorganic Bases. *Adv. Synth. Catal.* **2019**, *361*, 317−325.

(16) Song, B.; Qin, A. J.; Tang, B. Z. Green Monomer of CO_2 and Alkyne-Based Four-Component Tandem Polymerization toward Regio- and Stereoregular Poly(aminoacrylate)s. *Chinese J. Polym. Sci.* **2020**, *39*, 51−59.

(17) Song, B.; Zhang, R.; Hu, R.; Chen, X.; Liu, D.; Guo, J.; Xu, X.; Qin, A.; Tang, B. Z. Site-Selective, Multistep Functionalizations of CO_2-Based Hyperbranched Poly(alkynoate)s toward Functional Polymetric Materials. *Adv. Sci.* **2020**, *7*, 2000465.

(18) Grignard, B.; Gennen, S.; Jérôme, C.; Kleij, A. W.; Detrembleur, C. Advances in the Use of CO_2 as a Renewable Feedstock for the Synthesis of Polymers. *Chem. Soc. Rev.* **2019**, *48*, 4466−4514.

(19) Song, B.; Qin, A.; Tang, B. Z. New Polymerizations Based on Green Monomer of Carbon Dioxide. *Acta Chim. Sin.* **2020**, *78*, 9−22.

(20) Song, B.; Bai, T. W.; Liu, D. M.; Hu, R.; Lu, D.; Qin, A. J.; Ling, J.; Tang, B. Z. Visualized Degradation of CO_2-based Unsaturated Polyesters toward Structure Controllable and High-value-added Fluorophores. *CCS Chem.* **2021**, *3*, 499−511.

(21) Nakano, R.; Ito, S.; Nozaki, K. Copolymerization of Carbon Dioxide and Butadiene via a Lactone Intermediate. *Nat. Chem.* **2014**, *6*, 325−331.

(22) Liu, M.; Sun, Y.; Liang, Y.; Lin, B. L. Highly Efficient Synthesis of Functionalizable Polymers from a CO_2/1,3-Butadiene-Derived Lactone. *ACS Macro Lett.* **2017**, *6*, 1373−1378.

(23) Zhang, Y.; Xia, J.; Song, J.; Zhang, J.; Ni, X.; Jian, Z. Combination of Ethylene, 1,3-Butadiene, and Carbon Dioxide into Ester-Functionalized Polyethylenes via Palladium-Catalyzed Coupling and Insertion Polymerization. *Macromolecules* **2019**, *52*, 2504−2512.

(24) Gennen, S.; Grignard, B.; Tassaing, T.; Jérôme, C.; Detrembleur, C. CO_2-Sourced α-Alkylidene Cyclic Carbonates: A

Step Forward in the Quest for Functional Regioregular Poly(urethane)s and Poly(carbonate)s. *Angew. Chem., Int. Ed.* **2017**, *56*, 10394−10398.
(25) Ouhib, F.; Grignard, B.; Van Den Broeck, E.; Luxen, A.; Robeyns, K.; Van Speybroeck, V.; Jerome, C.; Detrembleur, C. A Switchable Domino Process for the Construction of Novel CO_2-Sourced Sulfur-Containing Building Blocks and Polymers. *Angew. Chem., Int. Ed.* **2019**, *58*, 11768−11773.
(26) Tsuda, T.; Maruta, K.; Kitaike, Y. Nickel(0)-Catalyzed Alternating Copolymerization of Carbon Dioxide with Diynes to Poly(2-pyrones). *J. Am. Chem. Soc.* **1992**, *114*, 1498−1499.
(27) Tsuda, T.; Maruta, K. Nickel(0)-Catalyzed Alternating Copolymerization of 2,6-Octadiyne with Carbon Dioxide to Poly(2-pyrone). *Macromolecules* **1992**, *25*, 6102−6105.
(28) Teffahi, D.; Hocine, S.; Li, C. J. Synthesis of Oxazolidinones, Dioxazolidinone and Polyoxazolidinone (a New Polyurethane) via a Multi Component-Coupling of Aldehyde, Diamine Dihydrochloride, Terminal Alkyne and CO_2. *Lett. Org. Chem.* **2012**, *9*, 585−593.
(29) Fu, W.; Dong, L.; Shi, J.; Tong, B.; Cai, Z.; Zhi, J.; Dong, Y. Multicomponent Spiropolymerization of Diisocyanides, Alkynes and Carbon Dioxide for Constructing 1,6-Dioxospiro[4,4]nonane-3,8-diene as Structural Units under One-Pot Catalyst-Free Conditions. *Polym. Chem.* **2018**, *9*, 5543−5550.
(30) Song, B.; Bai, T.; Xu, X.; Chen, X.; Liu, D.; Guo, J.; Qin, A.; Ling, J.; Tang, B. Z. Multifunctional Linear and Hyperbranched Five-Membered Cyclic Carbonate-Based Polymers Directly Generated from CO_2 and Alkyne-Based Three-Component Polymerization. *Macromolecules* **2019**, *52*, 5546−5554.
(31) Lygin, A. V.; de Meijere, A. Isocyanides in the Synthesis of Nitrogen Heterocycles. *Angew. Chem., Int. Ed.* **2010**, *49*, 9094−9124.
(32) Kruithof, A.; Ruijter, E.; Orru, R. V. A. Synthesis of Heterocycles by Formal Cycloadditions of Isocyanides. *Chem. − Asian J.* **2015**, *10*, 508−520.
(33) Nair, V.; Rajesh, C.; Vinod, A. U.; Bindu, S.; Sreekanth, A. R.; Mathen, J. S.; Balagopal, L. Strategies for Heterocyclic Construction via Novel Multicomponent Reactions Based on Isocyanides and Nucleophilic Carbenes. *Acc. Chem. Res.* **2003**, *36*, 899−907.
(34) Jiang, B.; Rajale, T.; Wever, W.; Tu, S. J.; Li, G. Multicomponent Reactions for the Synthesis of Heterocycles. *Chem. − Asian J.* **2010**, *5*, 2318−2335.
(35) Váradi, A.; Palmer, T.; Notis Dardashti, R.; Majumdar, S. Isocyanide-Based Multicomponent Reactions for the Synthesis of Heterocycles. *Molecules* **2015**, *21*, 19.
(36) Mampuys, P.; Neumann, H.; Sergeyev, S.; Orru, R. V. A.; Jiao, H.; Spannenberg, A.; Maes, B. U. W.; Beller, M. Combining Isocyanides with Carbon Dioxide in Palladium-Catalyzed Heterocycle Synthesis: *N*3-Substituted Quinazoline-2,4(1*H*,3*H*)-Diones via a Three-Component Reaction. *ACS Catal.* **2017**, *7*, 5549−5556.
(37) Xu, P.; Wang, F.; Wei, T. Q.; Yin, L.; Wang, S. Y.; Ji, S. J. Palladium-Catalyzed Incorporation of Two C1 Building Blocks: The Reaction of Atmospheric CO_2 and Isocyanides with 2-Iodoanilines Leading to the Synthesis of Quinazoline-2,4(1*H*,3*H*)-Diones. *Org. Lett.* **2017**, *19*, 4484−4487.
(38) Zhang, W. Z.; Li, H.; Zeng, Y.; Tao, X.; Lu, X. Palladium-Catalyzed Cyclization Reaction of *o*-Haloanilines, CO_2 and Isocyanides: Access to Quinazoline-2,4(1*H*,3*H*)-Diones. *Chin. J. Chem.* **2018**, *36*, 112−118.
(39) Dahlenburg, L.; Treffert, H.; Heinemann, F. W. 1,3-Bis(α-aminoisopropyl)benzene, *Meta*-$C_6H_4(CMe_2NH_2)_2$: An *N*,*N*-Bridging and *N*,*C*,*N*-Cyclometalating Ligand. *Inorg. Chim. Acta* **2008**, *361*, 1311−1318.
(40) Tian, T.; Hu, R.; Tang, B. Z. Room Temperature One-Step Conversion from Elemental Sulfur to Functional Polythioureas through Catalyst-Free Multicomponent Polymerizations. *J. Am. Chem. Soc.* **2018**, *140*, 6156−6163.
(41) Hill, N. L.; Braslau, R. Synthesis and Characterization of a Novel Bisnitroxide Initiator for Effecting "Outside-In" Polymerization. *Macromolecules* **2005**, *38*, 9066−9074.
(42) Sunke, R.; Kumar, V.; Ashfaq, M. A.; Yellanki, S.; Medisetti, R.; Kulkarni, P.; Ramarao, E. V. V. S.; Ehtesham, N. Z.; Pal, M. A Pd(II)-Catalyzed C−H Activation Approach to Densely Functionalized *N*-Heteroaromatics Related to Neocryptolepine and Their Evaluation as Potential Inducers of Apoptosis. *RSC Adv.* **2015**, *5*, 44722−44727.
(43) Peng, X.; Zhu, L.; Hou, Y.; Pang, Y.; Li, Y.; Fu, J.; Yang, L.; Lin, B.; Liu, Y.; Cheng, M. Access to Benzo[*a*]carbazoles and Indeno[1,2-*c*]quinolines by a Gold(I)-Catalyzed Tunable Domino Cyclization of Difunctional 1,2-Diphenylethynes. *Org. Lett.* **2017**, *19*, 3402−3405.
(44) Gallagher, W. P.; Vo, A. Dithiocarbamates: Reagents for the Removal of Transition Metals from Organic Reaction Media. *Org. Process Res. Dev.* **2015**, *19*, 1369−1373.
(45) Seo, M.; Park, J.; Kim, S. Y. Self-Assembly Driven by an Aromatic Primary Amide Motif. *Org. Biomol. Chem.* **2012**, *10*, 5332−5342.
(46) Sherrington, D. C.; Taskinen, K. A. Self-Assembly in Synthetic Macromolecular Systems via Multiple Hydrogen Bonding Interactions. *Chem. Soc. Rev.* **2001**, *30*, 83−93.
(47) Feng, H. T.; Lam, J. W. Y.; Tang, B. Z. Self-Assembly of AIEgens. *Coord. Chem. Rev.* **2020**, *406*, 213142.
(48) Lou, X. Y.; Yang, Y. W. Aggregation-Induced Emission Systems involving Supramolecular Assembly. *Aggregate* **2020**, *1*, 19−30.
(49) Lee, M. T.; Ahmed, T.; Friedman, M. E. Inhibition of Hydrolytic Enzymes by Gold Compounds. I. β-Glucuronidase and Acid Phosphatase by Sodium Tetrachloroaurate (III) and Potassium Tetrabromoaurate (III). *J. Enzyme Inhib.* **1989**, *3*, 23−33.
(50) Nyarko, E.; Hara, T.; Grab, D. J.; Habib, A.; Kim, Y.; Nikolskaia, O.; Fukuma, T.; Tabata, M. In Vitro Toxicity of Palladium(II) and Gold(III) Porphyrins and Their Aqueous Metal Ion Counterparts on Trypanosoma Brucei Brucei Growth. *Chem.-Biol. Interact.* **2004**, *148*, 19−25.
(51) Zhang, J. F.; Zhou, Y.; Yoon, J.; Kim, J. S. Recent Progress in Fluorescent and Colorimetric Chemosensors for Detection of Precious Metal Ions (Silver, Gold and Platinum Ions). *Chem. Soc. Rev.* **2011**, *40*, 3416−3429.
(52) Doidge, E. D.; Carson, I.; Tasker, P. A.; Ellis, R. J.; Morrison, C. A.; Love, J. B. A Simple Primary Amide for the Selective Recovery of Gold from Secondary Resources. *Angew. Chem., Int. Ed.* **2016**, *55*, 12436−12439.
(53) Nam, S. H.; Lee, W. M.; Shin, Y. J.; Yoon, S. J.; Kim, S. W.; Kwak, J. I.; An, Y. J. Derivation of Guideline Values for Gold(III) Ion Toxicity Limits to Protect Aquatic Ecosystems. *Water Res.* **2014**, *48*, 126−136.

https://doi.org/10.1021/acs.macromol.1c00312
Macromolecules 2021, 54, 4112−4119